Modeling Plasma Detachment in Magnetized Exhaust Systems: Towards Plasma Detachment

Mikhail Khodak

Princeton Plasma Physics Laboratory, Princeton, New Jersey

Sponsored by the U.S. Department of Energy

August 2012

Introduction

Many fusion devices that have been developed or proposed as alternatives to tokamaks and other toroidal machines employ cylindrical structures and thus require exhaust systems to expel plasma particles from confinement chambers because it cannot be indefinitely looped in circles as plasma is in toroids. An important feature of the exhaust region is a magnetic field expanding outwardly from the aperture through which plasma flows, caused by the solenoids present around the nozzle. Generally, charged plasma particles moving along magnetic field lines will remain attached to the lines; thus, for the field lines in the exhaust system the particles will move increasingly in the radial direction away from the major axis of the cylinder as they move further from the nozzle. However, using MHD equations it has been shown theoretically that when the local kinetic energy of particles is greater than the local magnetic field energy plasma particles will detach from the field lines and continue in a direction more parallel to the major axis.[1] This detachment is very important for applications of devices such as the FRC and plasma-based rockets because more particles moving parallel to the access leads to greater exhaust efficiency and greater thrust. However, detachment has not yet been proven by experimental results. The aim of this report is to develop a sufficiently accurate and flexible model of the magnetic field outside a solenoid and then to use LSP, a PIC code written in C, to begin to investigate whether detachment does indeed occur and to see which magnetic field geometries lead to the best results.

Magnetic Field Model

The exhaust region consists of a set of coaxial solenoids through and out of which flows outwardly directed plasma particles. Because the question is to determine to see how charged particles detach from magnetic field lines, it is important to devise a model of the axial and radial field in all locations of the expansion region. Because much of this region lies outside the current-carrying coils or is near the edges of finite solenoids, basic formulas for the field of solenoids will not be adequate, so one derived from the integration of thin, current-carrying hoops will be used. Once derived, the equations will be put in Mathcad and numerically processed to give the magnetic field at desired points in the expansion region.

Derivation

The following derivations will reference the following variables:

$I \; is \; the \; current, assumed \; to \; be \; constant$

$J \; is \; the \; current \; density, assumed \; to \; be \; constant$

$\rho \; is \; the \; radius \; of \; a \; circular, current - carrying \; hoop$

$l \; is \; the \; axial \; position \; of \; a \; circular, current - carrying \; hoop$

$R \; is \; the \; inner \; radius \; of \; the \; coil$

$d \; is \; the \; radial \; thickness \; of \; the \; coil, such \; that \; R + d \; is \; the \; outer \; radius \; of \; the \; coil$

$L \; is \; the \; length \; of \; the \; solenoid$

$N \; is \; the \; number \; of \; turns \; in \; the \; solenoid$

$C \; is \; the \; axial \; position \; the \; center \; of \; the \; solenoid$

Assume that a solenoid is composed of a set of current-carrying hoops. Because the magnetic field of a uniformly thick solenoid is independent of angle, cylindrical coordinates will be used. The formula for the axial magnetic field of a single, thin, current-carrying hoop is: [2]

$$b_z = \frac{\mu_0 I}{2\pi\sqrt{(r+\rho)^2 + z^2}}\left[\frac{r^2 - \rho^2 - z^2}{(r-\rho)^2 + z^2}E(k) + K(k)\right]$$

$$s.t. \;\; k^2 = \frac{4r\rho}{(r+\rho)^2 + z^2}$$

$and \; E(k) and \; K(k) \; are \; complete \; elliptic \; integrals \; of \; the \; first \; and \; second \; kind, respectively,$

$$s.t. \; K(k) = \int_0^{\frac{\pi}{2}} \frac{d\theta}{\sqrt{1 - k^2 \sin^2\theta}} \; and \; E(k) = \int_0^{\frac{\pi}{2}} \sqrt{1 - k^2 \sin^2\theta}\, d\theta$$

The hoops must be integrated over length and radius in order to get a formula for a thick, finite solenoid. To do so, the axial formula for the hoop must be defined as a function of position, radius, and distance from the zero-coordinate on the axis:

$$b_z(z, r, \rho, l) = \frac{\mu_0 I}{2\pi\sqrt{(r+\rho)^2 + (z-l)^2}}\left[\frac{r^2 - \rho^2 - (z-l)^2}{(r-\rho)^2 + (z-l)^2}E(k) + K(k)\right],$$

$$s.t. \;\; k^2 = \frac{4r\rho}{(r+\rho)^2 + (z-l)^2}$$

Then:

$$db_z(z,r,\rho,l) = \frac{\mu_0 dI}{2\pi\sqrt{(r+\rho)^2+(z-l)^2}}\left[\frac{r^2-\rho^2-(z-l)^2}{(r-\rho)^2+(z-l)^2}E(k)+K(k)\right]$$

Substituting current density for current:

$JdA = dI, \qquad dA = dld\rho$
So:

$$db_z(z,r,\rho,l) = \frac{\mu_0 Jdld\rho}{2\pi\sqrt{(r+\rho)^2+(z-l)^2}}\left[\frac{r^2-\rho^2-(z-l)^2}{(r-\rho)^2+(z-l)^2}E(k)+K(k)\right]$$

Since current and current density is constant:

$$JA = I, A = \frac{d}{N}L$$

$$J = \frac{IN}{Ld}$$

Then:

$$db_z(z,r,\rho,l) = \frac{\mu_0 INdld\rho}{2\pi Ld\sqrt{(r+\rho)^2+(z-l)^2}}\left[\frac{r^2-\rho^2-(z-l)^2}{(r-\rho)^2+(z-l)^2}E(k)+K(k)\right]$$

Defining an integration function, which can be seen as the axial magnetic field density:

$$M_z(z,r,\rho,l) = \frac{\mu_0 IN}{2\pi Ld\sqrt{(r+\rho)^2+(z-l)^2}}\left[\frac{r^2-\rho^2-(z-l)^2}{(r-\rho)^2+(z-l)^2}E(k)+K(k)\right],$$

So:

$$B_z(z,r) = \int_R^{R+d}\int_{-\frac{L}{2}}^{\frac{L}{2}} M_z(z,r,\rho,l)dld\rho$$

$B_z(z,r)$ *gives the equation of the magnetic field in the axial direction at any coordinate* (z,r)

The radial magnetic field of a thin current-carrying hoop is given by:

$$b_r = \frac{\mu_0 Iz}{2\pi r\sqrt{(r+\rho)^2+z^2}}\left[\frac{r^2+\rho^2+z^2}{(r-\rho)^2+z^2}E(k)-K(k)\right]$$

Using a procedure similar to the one above, the radial magnetic field density can be defined and integrated:

$$M_r(z,r,\rho,l) = \frac{\mu_0 IN(z-l)}{2\pi L dr\sqrt{(r+\rho)^2+(z-l)^2}}\left[\frac{r^2+\rho^2+(z-l)^2}{(r-\rho)^2+(z-l)^2}E(k)-K(k)\right]$$

So:

$$B_r(z,r) = \int_R^{R+d}\int_{-\frac{L}{2}}^{\frac{L}{2}} M_r(z,r,\rho,l)\,dl\,d\rho$$

For a solenoid located at a specific axial position, the field is given by:

$$\boldsymbol{B}(z,r) = \langle \int_R^{R+d}\int_{-\frac{L}{2}}^{\frac{L}{2}} M_z(z-C,r,\rho,l)\,dl\,d\rho\,,\ \int_R^{R+d}\int_{-\frac{L}{2}}^{\frac{L}{2}} M_r(z-C,r,\rho,l)\,dl\,d\rho\rangle$$

By superposition, the field created by *n* solenoids located on the same axis, given the spatial and current parameters of each, will be:

$$\boldsymbol{B_{1,2,\ldots,n}}(z,r) = \boldsymbol{B_1}(z,r,I_1,R_1,d_1,L_1,N_1,C_1) + \boldsymbol{B_2}(z,r,I_2,R_2,d_2,L_2,N_2,C_2) + \cdots + \boldsymbol{B_n}(z,r,I_n,R_n,d_n,L_n,N_n,C_n)$$

Using this equation, the magnetic field of the expansion region of any axial-symmetric exhaust system can be modeled.

Advantages and Limitations of the Model

Numerical computations of the field at specific points and graphical output agree well with basic qualitative knowledge of magnetic fields of solenoids (Fig. 1 & 2). Although it is difficult to check the validity of the model off-axis, the model compares very favorably with a radial integration of an independently-derived for the axial magnetic field of a thin solenoid on-axis (Fig. 3).[3] An important advantage of the model is the ease of adding more solenoids so long as they are on the same axis, a condition met in basic plasma exhaust systems.

Many of the limitations of using the model stem from its use with MathCad rather than known mathematical inconsistencies. The program has an allowable integration error of up to 10G and often fails to converge to solutions at specific points. Future use of the model should employ other mathematical programs or simplify the model for better results in MathCad.

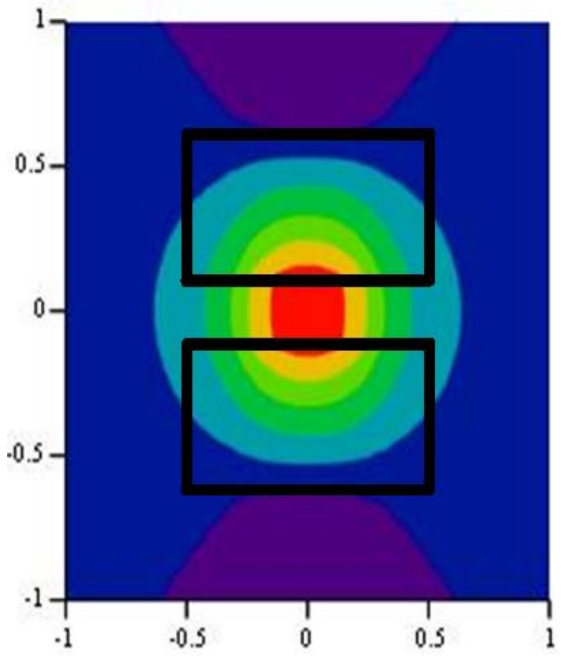

Figure 1

B_z in the plane of a 50cm long solenoid with a 10cm inner radius, 70cm outer radius, 10 turns, and a 400A current. Axes coordinates are in meters.

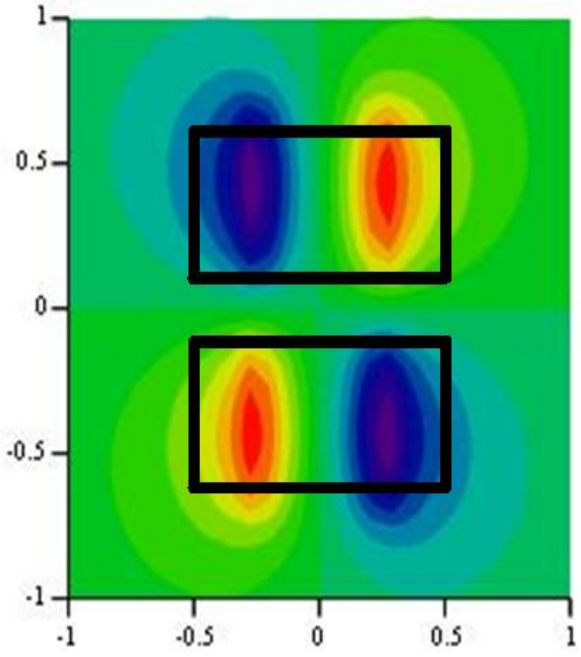

Figure 2

B_r in the plane of the same solenoid as Fig. 1.

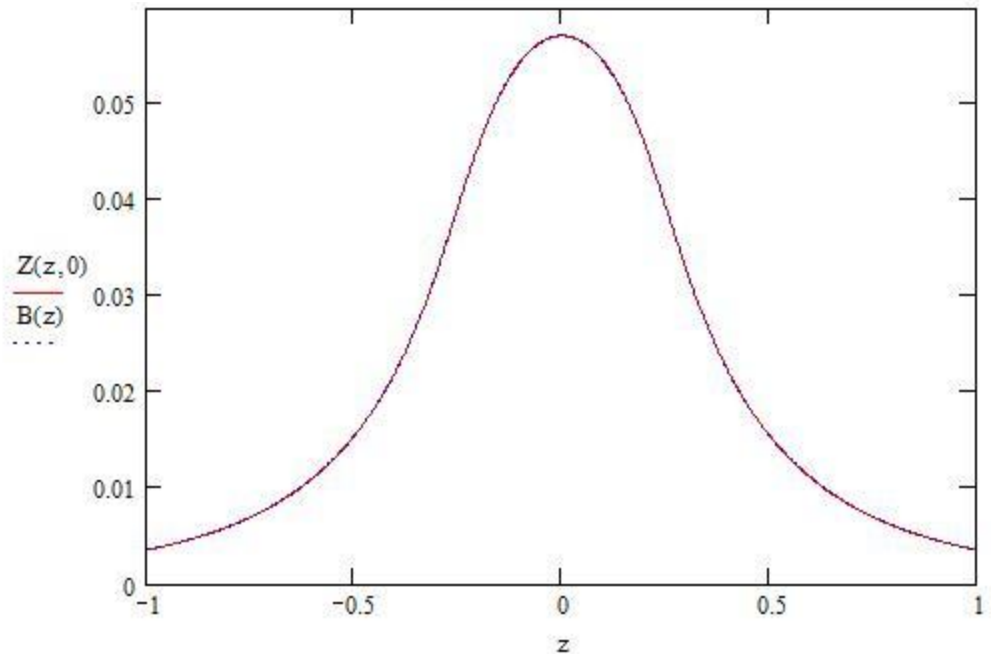

Figure 3

Comparison of model axial magnetic field along the z-axis (Z(z,0)) to exact solution of on-axis magnetic field of a thick solenoid given (B(z)) given by

$$B_z(z) = \frac{\mu_0 IN}{4L}\left[(L-2z)\log\left(\sqrt{L^2-4Lz+4(\rho^2+z^2)}+2\rho\right)+(L+2z)\log\left(\sqrt{L^2+4Lz+4(\rho^2+z^2)}+2\rho\right)\right]\Bigg|_{R}^{R+d}$$

Simulation of Plasma Detachment in LSP

Theory

Ideal MHD models of plasma expansion out of magnetized nozzles have predicted that plasma detachment, the stretching of field lines to the infinity by the plasma, will occur when the kinetic energy of the plasma is greater than the local magnetic field energy. Therefore, in simulating the detachment region the goal is to create a region where the magnetic field is very small and the curvature of the magnetic field lines very high so particles can detach due to their velocity along the axis. The ratio of kinetic energy to magnetic field energy will further be increased by the acceleration of ions caused by the electric field created by electrons, which move ahead of the ions into the region due to their greater energy. [4]

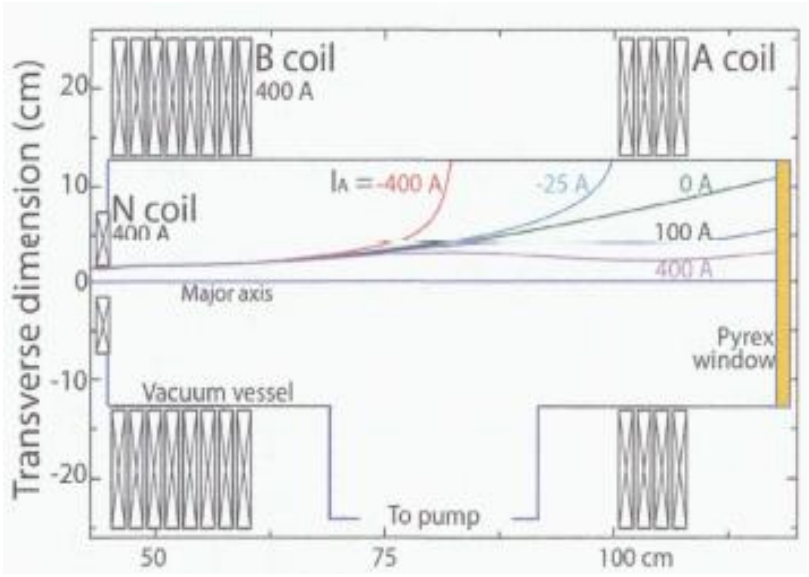

Figure 4

Magnetic field line curvature comparisons of different fields created by varying the magnitude of the A-coil current (I_A).

Expansion Field

A region of very low magnetic field energy was created using an arrangement of three solenoids, two around the aperture, both with currents of 400A, and another further away along the z-axis with a varying negative current. Although in further discussion the negative current will be -400A, other field configurations of interest have been achieved with -25A (Fig. 4). The coil parameters are given in Table 1 and the resulting axial and radial field strengths, magnetic field energy, and magnetic field streamlines as output from LSP is also given (Fig. 5-8). The maximum field strength is about 6000G, with the axial magnetic field zero at about z=38cm.

Table 1			
	Nozzle Coil (N)	Coil B	Reverse Coil (A)
Current (I)	400 A	400 A	-400 A
Length (L)	1.9 cm	11.5 cm	5.8 cm
Thickness (d)	4.5 cm	11.9 cm	11.9 cm
Radius (R)	1.3 cm	13.0 cm	13.0 cm
Number of Turns (N)	36	264	132
Axial Position (C)	.95 cm	7.0 cm	59.5 cm

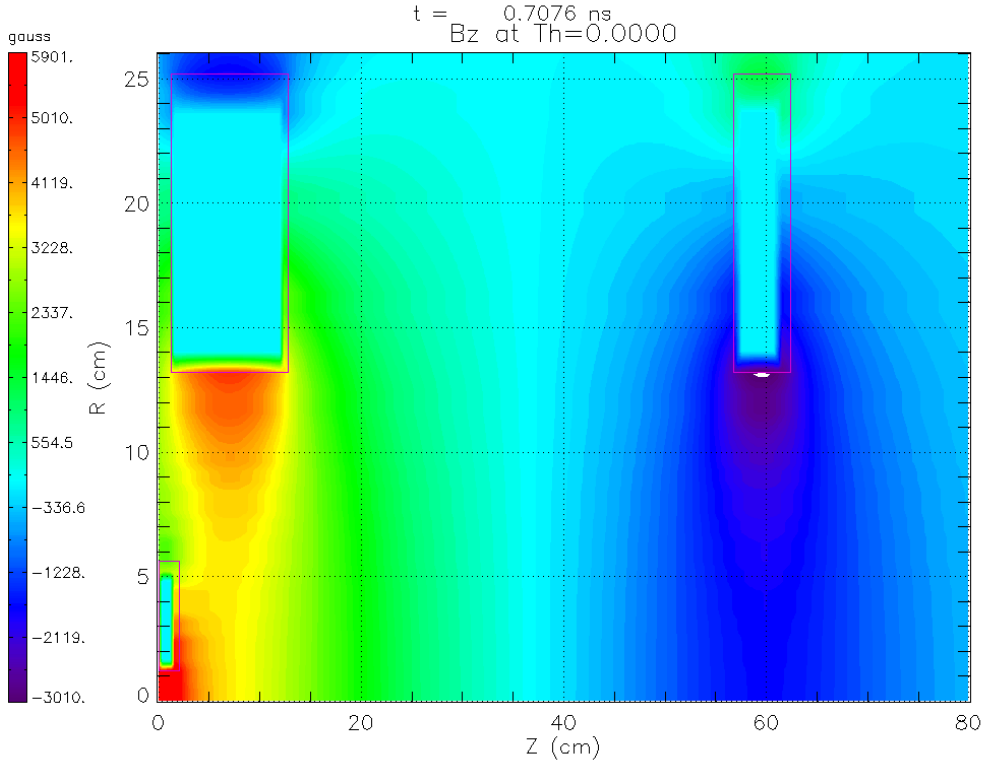

Figure 5

Initial axial magnetic field. The coils are depicted by the outlined boxes.

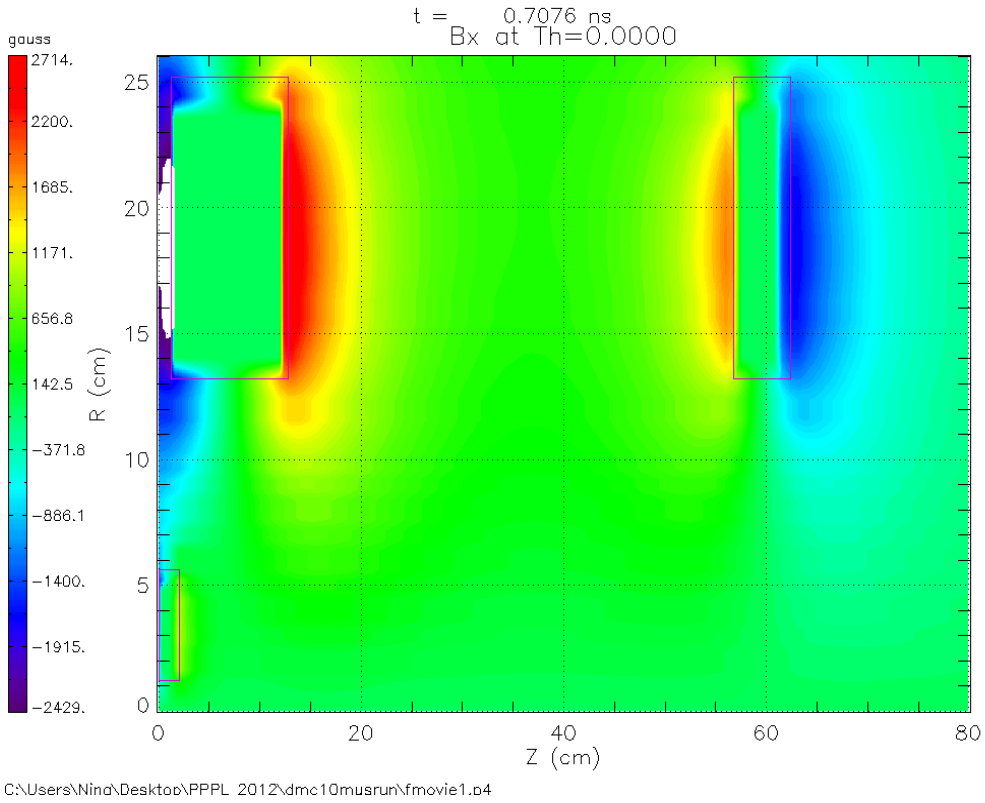

Figure 6

Initial radial magnetic field. The coils are depicted by the outlined boxes.

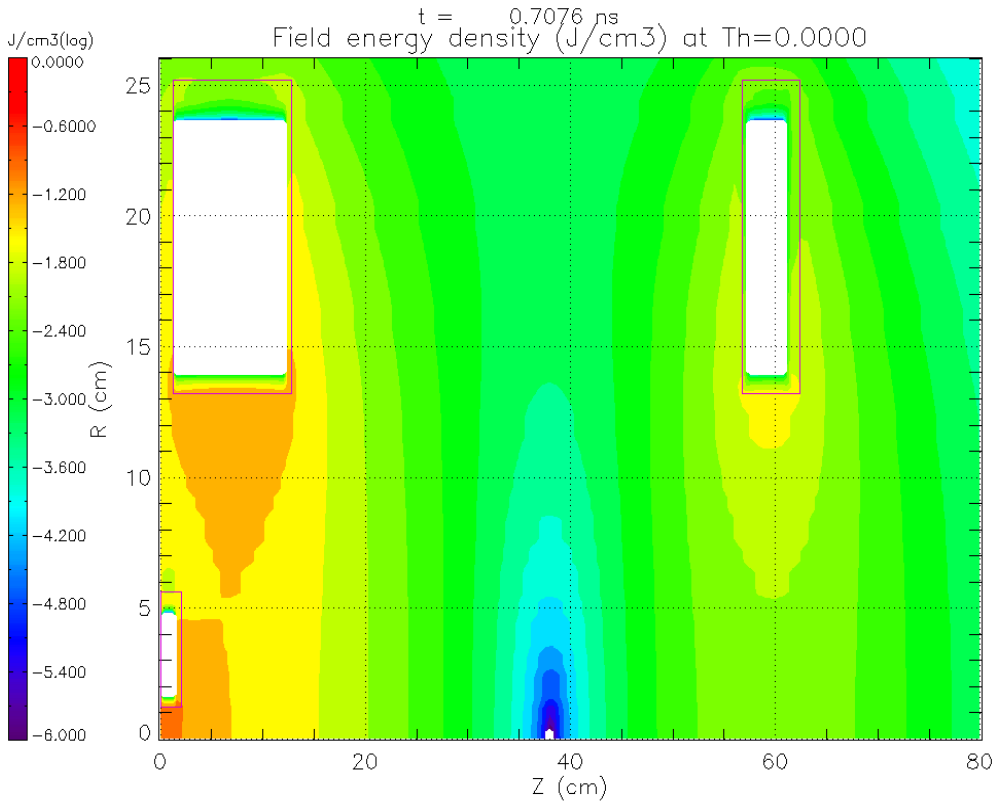

Figure 7

Initial magnetic field energy density, shown using a logarithmic scale. The field energy is nearly zero on-axis at z=38cm.

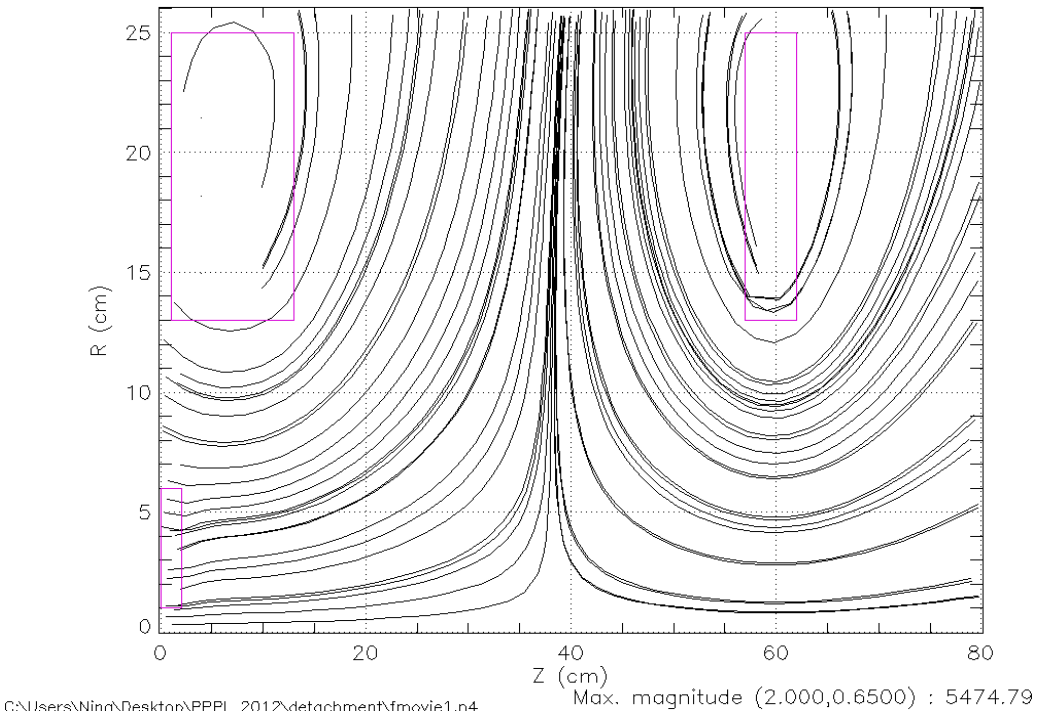

Figure 8

Initial magnetic field streamlines, showing the cusp shape of the field at z=38cm.

Simulating in LSP

LSP is a Particle-In-Cell code written in C that uses superparticles to represent plasma particles moving in given fields and geometries. Plasma and field parameters are given at the beginning of simulations and the program solves for dynamic changes in the field due to particle movements without outside directives. Timesteps in the program are either manually set or determined by setting the Courant multiplier, which is a parameter that ensures that particles do not travel more than a grid length in one timestep. The smaller the courant multiplier, which can be anywhere from 0 to 1, the smaller the timesteps will be.

1st LSP Simulation

An initial LSP simulation was run using the parameters given in Table 2. Although the aperture plasma density of $10^9 cm^{-3}$ is three orders of magnitude less than that which will eventually be desired in actual plasma exhaust systems, the lower density is thought to increase the accuracy of the simulation by increasing the plasma's Debye length and electron gyroradius to better compare with the grid size. Due to the low resolution of the initial run, the simulation was run for 4 microseconds.

Table 2	
Parameter	Value
Plasma Injection Velocity	Mach 1 (20100 m/s)
Plasma Density	$10^9 cm^{-3}$
Electron Energy	5 eV
Ion (H+) Energy	1 eV
Grid Area	80 cm x 26 cm
Number of Cells	6750
Aperture Grid Resolution	.4 cm x .4 cm
Courant Multiplier	.75
Time	4 microseconds
Number of Processors	1

The results of the run showed that electrons did move ahead of the protons and create a positive magnetic field in the axial direction, with some detaching and some traveling into the cusp (Fig. 9-11). However, once protons moved past the aperture region they underwent unrealistic levels of heating, exhibited standing wave behavior, and seemed to prevent electrons from traveling along the z-axis. With very high temperatures, the ions all detached and moved through the reverse coil (Fig. 12-14).

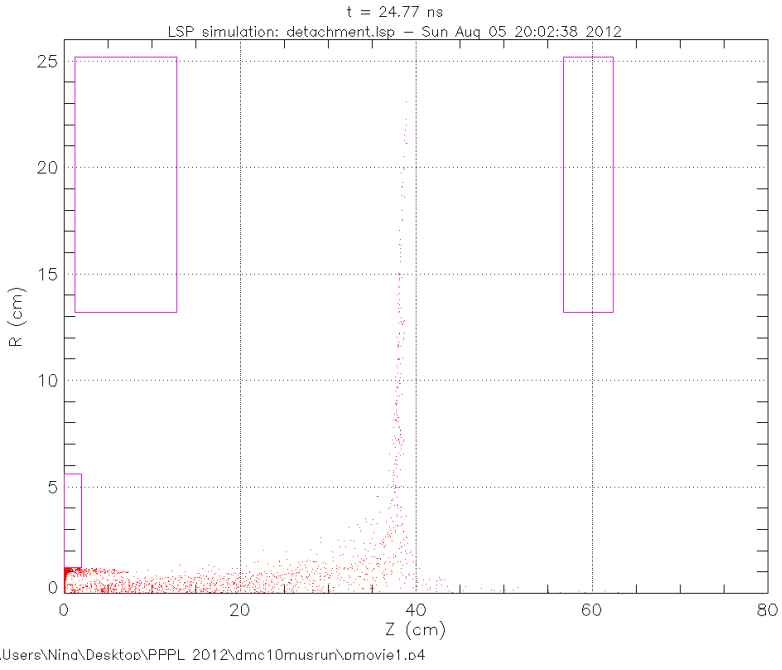

Figure 9

Particles in the expansion region at 25ns. Red dots are electrons, blue dots are ions.

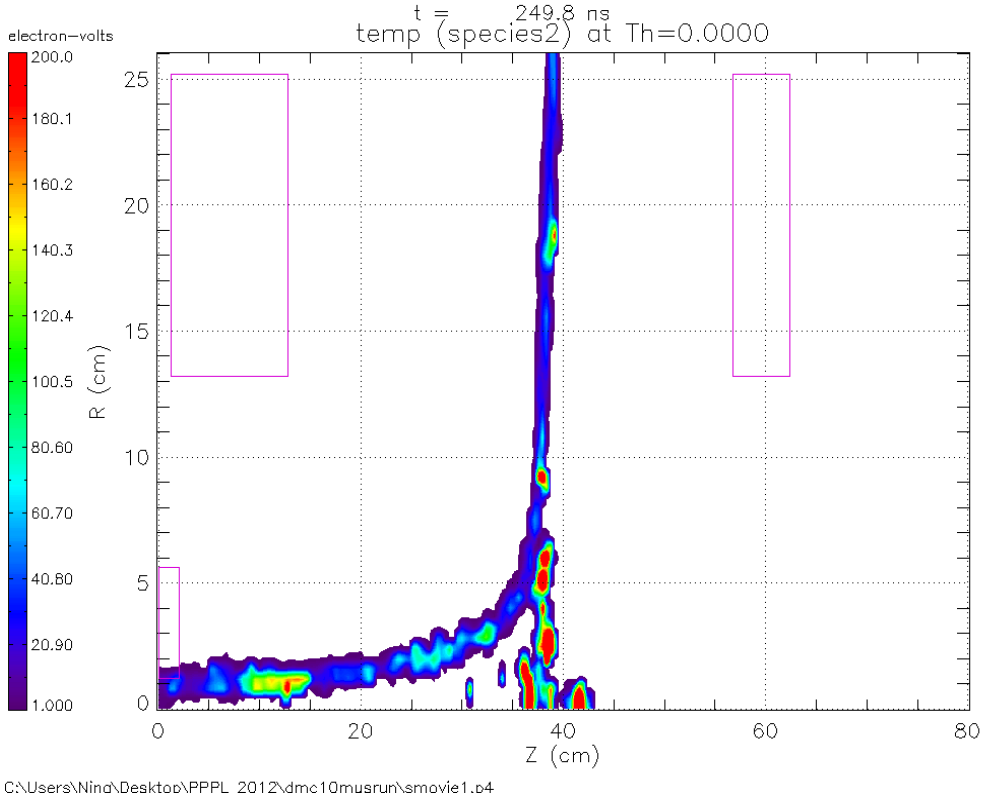

Figure 10

Hot electrons moving through the detachment region (electron temperature at 246ns).

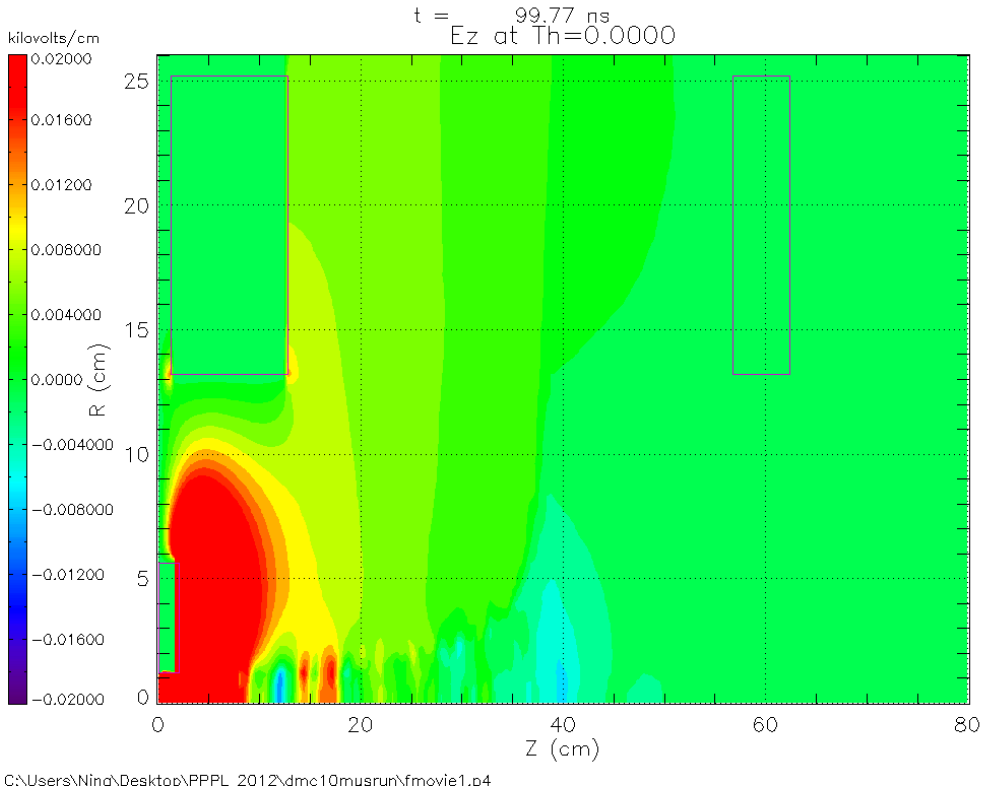

Figure 11

Axial electric field at 100ns

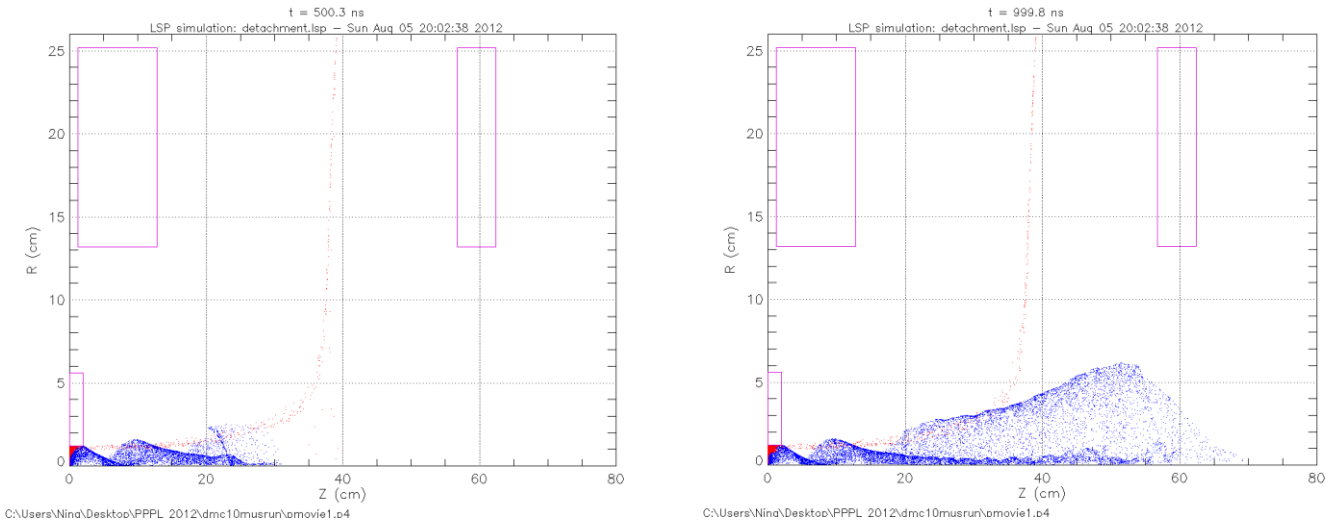

Figure 12

Particles at 500ns and 1000ns, with standing ion waves and the complete absence of electrons along the axis.

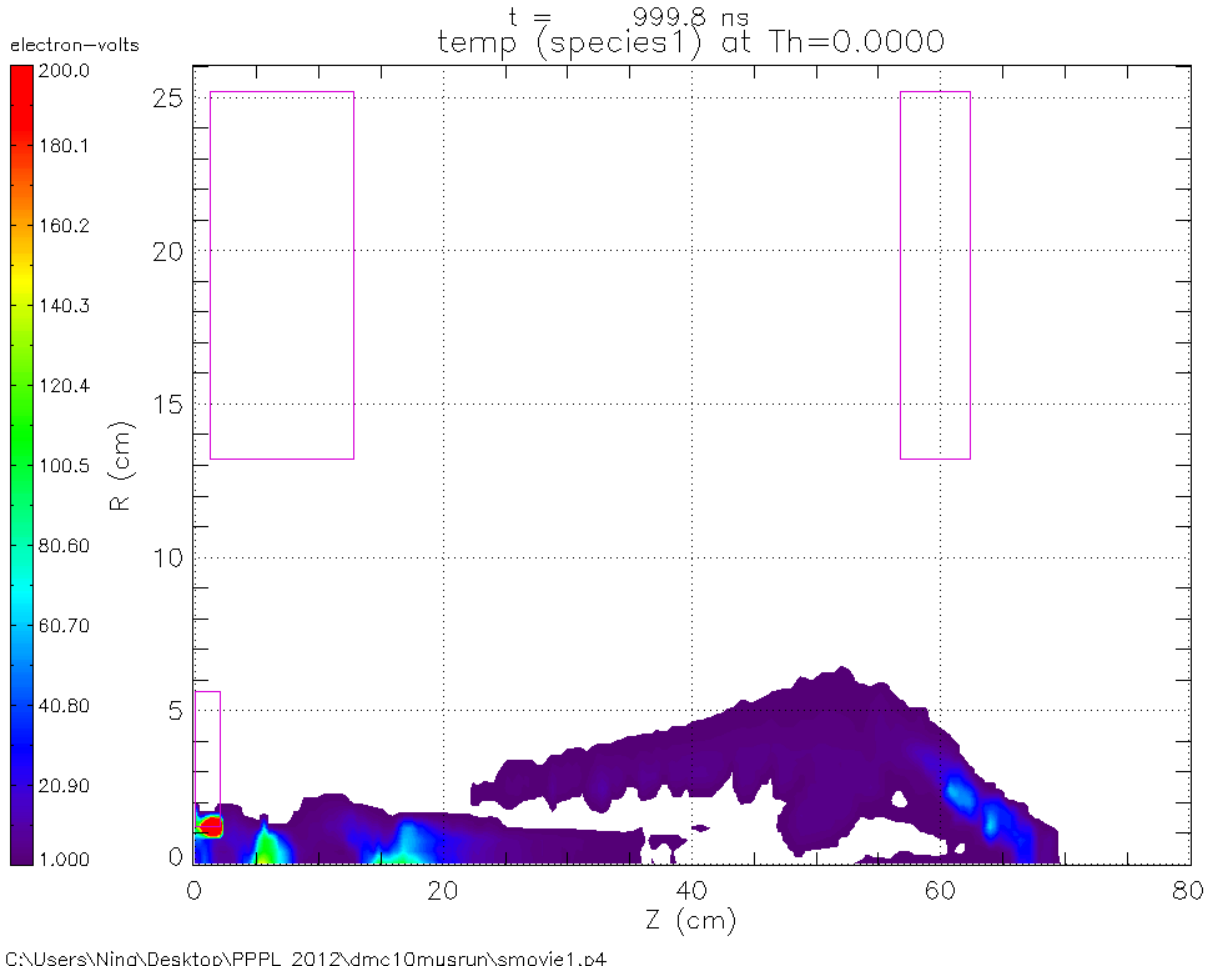

Figure 13

Ion temperature at 1000ns

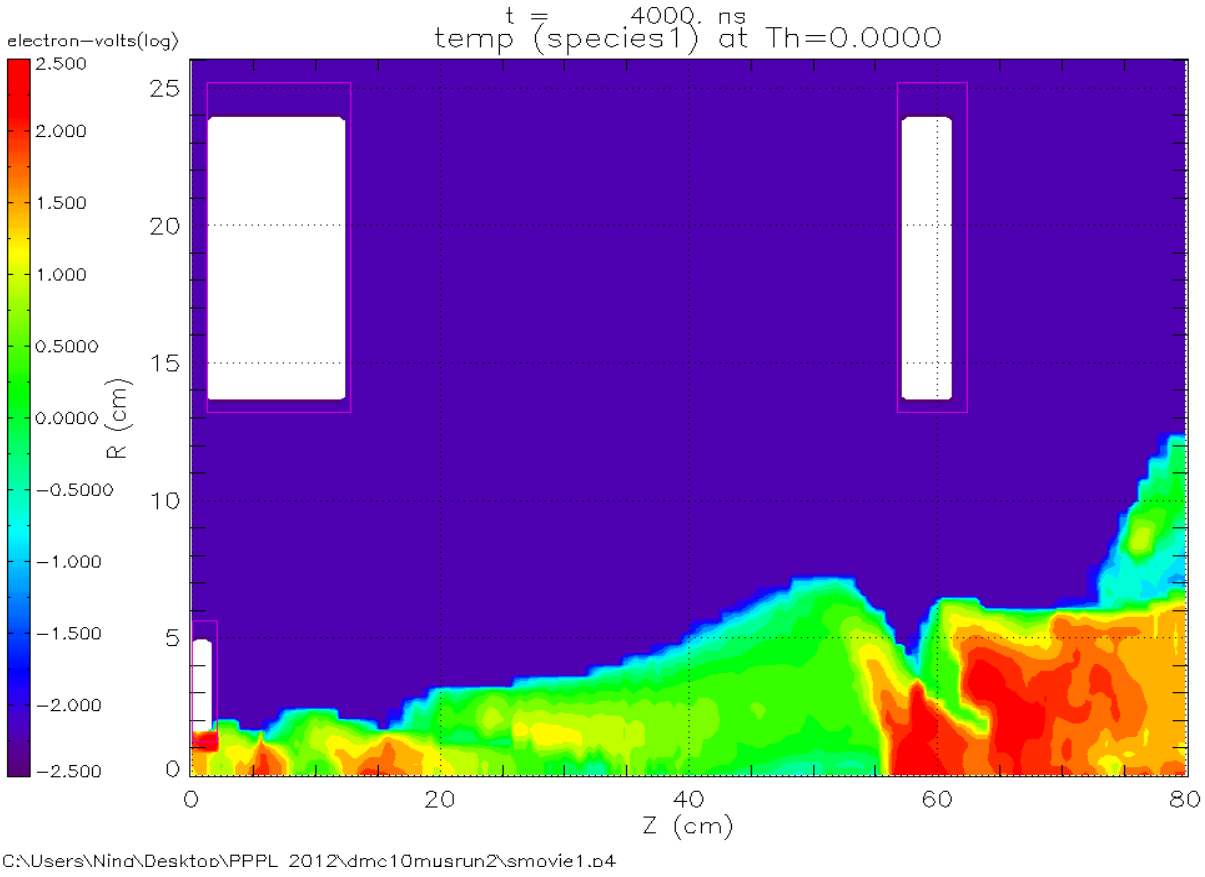

Figure 14

Ion temperature at 4 microseconds using a logarithmic scale.

2nd LSP Simulation

The second simulation employed a much smaller grid size in order to allow for the size of the gyroradii of the particles and the plasma Debye length. The resulting tenfold increase in the number of superparticles emitted per timestep and almost 100-fold increase in the number of cells greatly increased the time it took to conduct runs, so the simulation was run for only 246 nanoseconds (Table 3).

Table 3	
Parameter	Value
Plasma Injection Velocity	Mach 1 (20100 m/s)
Plasma Density	$10^{10} cm^{-3}$
Electron Energy	5 eV
Ion (H+) Energy	1 eV
Grid Area	80 cm x 26 cm
Number of Cells	600000
Aperture Grid Resolution	.04 cm x .04 cm
Courant Multiplier	.75
Time	246 nanoseconds
Number of Processors	64

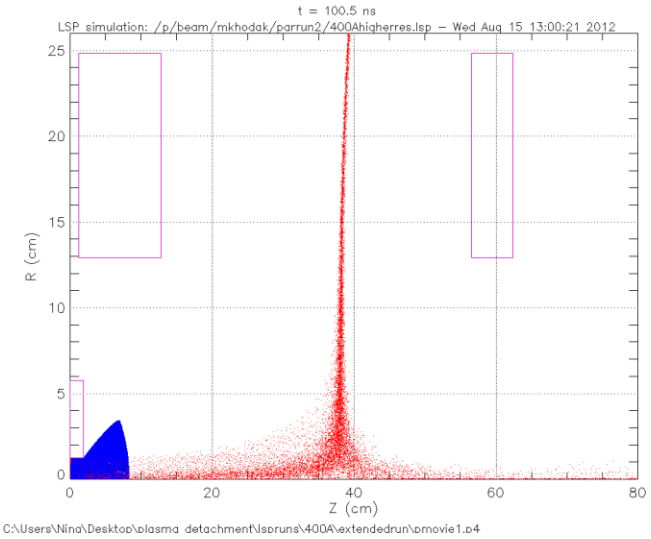

Figure 15

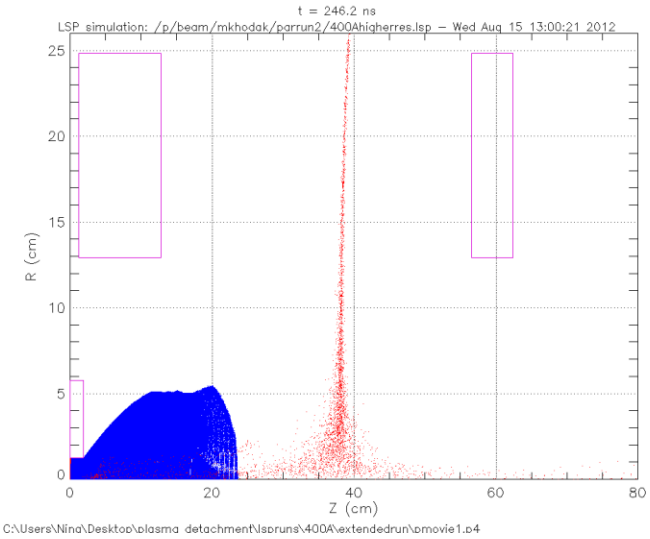

Figure 16

The higher-resolution simulation showed similar initial electron movements (Fig. 15). However, the protons, although heated to high temperatures near the aperture, cooled swiftly after moving further downstream to temperatures below the initial 1 eV given (Fig. 17-18). A conflicting observation was the rapid expansion of the ion-stream radius to 5cm almost immediately after protons left the aperture, pointing instead to much higher temperatures than those observed (Fig. 16).

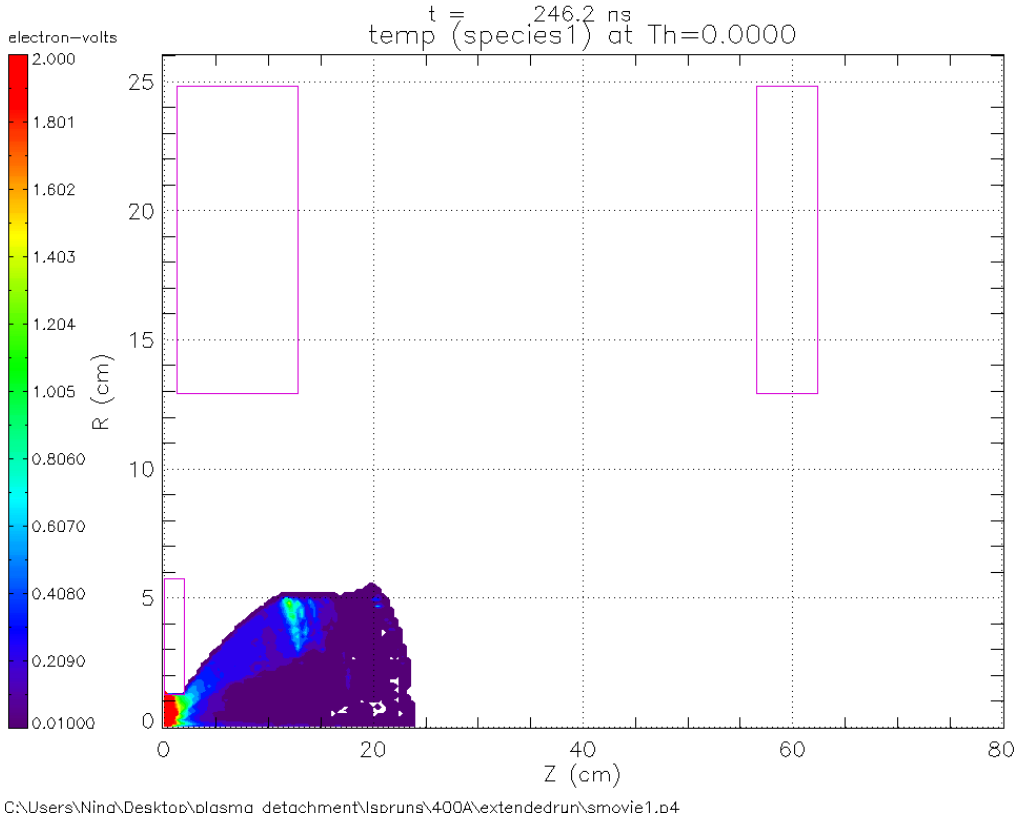

Figure 17

Ion temperature at 246ns

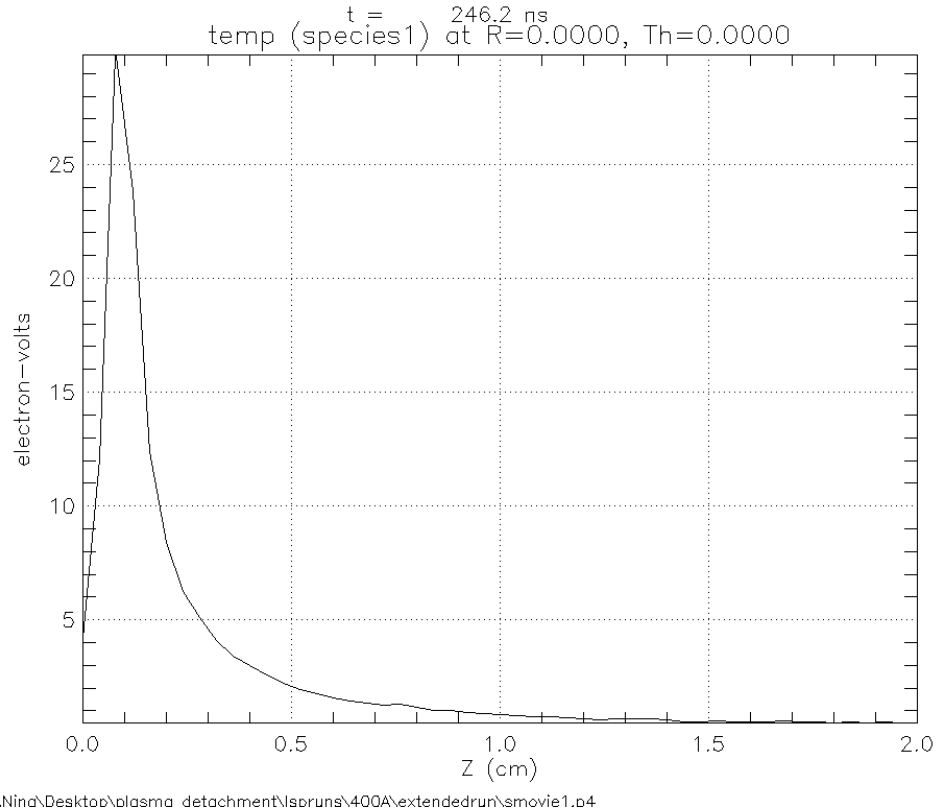

Figure 18

Axial ion temperature at 246ns

Continuing LSP Investigation

Simulations run in LSP thus far have yielded multiple problems in their compatibility with expected results. Future investigations will focus on using better grid and particle injection parameters to find scenarios that do not produce large ion heating variations or unrealistic speeds. Doing so will also require finding parameters that produce simulation results more quickly while maintaining model accuracy, especially by reducing the number of super-particles and increasing the courant multiplier while maintaining high grid resolution. Other alternatives include using a Cartesian rather than a Cylindrical coordinate system and testing alternate magnetic field geometries. The main focus of these inquiries will be to reconcile LSP simulations with basic theoretical results and from there conduct further experiments to arrive at a better understanding of optimal magnetic conditions for detachment.

Conclusion

A theoretical model for the magnetic field due to a set of coaxial solenoids was developed and numerically implemented in MathCad for the field configuration of a plasma exhaust system. In order to test detachment testing, a configuration using a reverse coil was used to increase the magnetic field line curvature. The resulting field was used in LSP simulations run to test parameters for further simulation of detachment in exhaust plasmas, resulting in many problems including rapid ion heating, fast particle speeds, and unexpected particle behavior outside of the aperture.

Acknowledgements

Project Supervisor:

- Samuel Cohen, PPPL

Advice:

-Clayton Myers, PPPL

- Andrei Khodak ,PPPL

-Erinc Tokluoglu, PPPL

-Dale Welch, Voss Scientific

-Christopher Mostrom, Voss Scientific

References

[1] A. V. Arefiev and B. N. Breizman, Phys. Plasmas **12**, 043504 (2005)

[2] Stewart, Joseph V. *Intermediate Electromagnetic Theory*. London: World Scientific Publishing Co. Pte. Ltd., 2001. 275-276. Print.

[3] Stratton, Julius Adams. *Electromagnetic Theory*. York, PA: McGraw-Hill Book Company, Inc., 1941. 233. Print.

[4] A. B. Sefkow and S. A. Cohen, Phys. Plasmas **16**, 053501 (2009)